RSC Advances

ROYAL SOCIETY OF CHEMISTRY

www.rsc.org/advances

RSC Advances

RSCPublishing

COMMUNICATION

Enhanced Emission from ZnO-Based Double Heterostructure Light-Emitting Devices Using a Distributed Bragg Reflector

Cite this: DOI: 10.1039/x0xx00000x

Ying-Jie Lu,[ab] Chong-Xin Shan,*[a] Ming-Ming Jiang,[a] Bing-Hui Li,[a] Ke-Wei Liu,[a] Rui-Gang Li,[c] and De-Zhen Shen*[a]

Received 00th January 2014,
Accepted 00th January 2014

DOI: 10.1039/x0xx00000x

www.rsc.org/

Double hetero-structured *n*-$Mg_{0.13}Zn_{0.87}O$/*i*-ZnO/*p*-$Mg_{0.13}Zn_{0.87}O$ light-emitting devices (LEDs) have been fabricated, and the *p*-type $Mg_{0.13}Zn_{0.87}O$ layer was obtained via a lithium-nitrogen codoping method. Obvious emission at around 400 nm has been observed from the LEDs under the drive of forward bias. To increase the light extraction from the LEDs, a distributed Bragg reflector whose reflectivity is 98% at 400 nm has been bonded backside the device, and the emission of the device has been enhanced by around 1.6 times with the reflector.

Introduction

The large exciton binding energy (60 meV) of ZnO suggests that efficient excitonic emission may be realized, thus a variety of potential applications in lighting, displaying, signalling, *etc*. may be expected from ZnO.[1-4]. Although much attention has been paid, the reports on efficient ZnO-based light-emitting devices (LEDs) are still rare in recent years, and most of them are realized in simple *p*-ZnO/*n*-ZnO structures.[5-10] It is accepted that in the *p*-ZnO/*n*-ZnO structures, since the mobility of electrons are usually larger than that of holes, the electrons and holes tend to recombine in the *p*-type ZnO region. While there are many residual donor-related defects and introduced acceptor-related defects in this layer, as a result, emission from donor-acceptor pairs usually dominates the emission of *p*-ZnO/*n*-ZnO structures.[6,9,10] By employing MgZnO/ZnO heterostructures the recombination region of electrons and holes can be confined into the ZnO layer, and the excitonic near-band-edge emission of ZnO can be obtained.[11,12] Nevertheless, very few reports on ZnO-based heterostructure LEDs can be found up to date, and most of which are focused on single-heterostructures,[11,13-16] while the reports on double heterostructure ZnO LEDs are still rare.[17-21]

In this communication, *n*-$Mg_{0.13}Zn_{0.87}O$/*i*-ZnO/*p*-$Mg_{0.13}Zn_{0.87}O$ double heterstructured LEDs have been constructed, in which the *p*-type $Mg_{0.13}Zn_{0.87}O$ layer was obtained by employing Li and N codoping method. Obvious emission at around 400 nm has been observed from the LEDs under the injection of continuous current. To increase the emission of the LEDs, a distributed Bragg reflector (DBR) whose reflectivity is about 98% at around 400 nm has been bonded onto the backside of the LEDs. It is found that the emission of the LEDs can be increased significantly.

Experimental

The *n*-$Mg_{0.13}Zn_{0.87}O$/*i*-ZnO/*p*-$Mg_{0.13}Zn_{0.87}O$ double heterostructures were grown by plasma-assisted molecular beam epitaxy technique (VG V80H), and *a*-plane sapphire was employed as a substrate. Lithium and nitrogen have been used to synthesize *p*-type ZnO based materials.[22-26] In this communication, we use Li and N codoping method to obtain *p*-type MgZnO. The detailed growth conditions for the *n*-MgZnO and *p*-MgZnO can be found elsewhere.[27] Metallic zinc, lithium and magnesium contained in individual Knudsen effusion cells were used as the Zn, Li and Mg source. Nitric oxide (NO) was used as N and O sources for the growth of the *p*-$Mg_{0.13}Zn_{0.87}O$ layer and oxygen (O_2) was used as O source for intrinsic ZnO (*i*-ZnO) and *n*-$Mg_{0.13}Zn_{0.87}O$. The gas sources were activated by an Oxford Applied Research HD25 radio-frequency (13.56 MHz) atomic source at a power of 300 W. The pressure in the growth chamber was fixed at 2×10^{-5} mbar, and the flow rate of NO and O_2 at 0.88 and 1.0 sccm during the growth process. The sapphire substrate was pretreated at 400 ^{o}C for 30 min to remove the possible surface contaminant. A ZnO film was employed to buffer the growth of the *n*-$Mg_{0.13}Zn_{0.87}O$/ZnO/*p*-$Mg_{0.13}Zn_{0.87}O$ double heterostructures. The substrate temperature was kept at 650 ^{o}C during the growth of the *n*-

$Mg_{0.13}Zn_{0.87}O$ and *p*-$Mg_{0.13}Zn_{0.87}O$ layer, while it was kept at 750 °C for the growth of the *i*-ZnO layer.

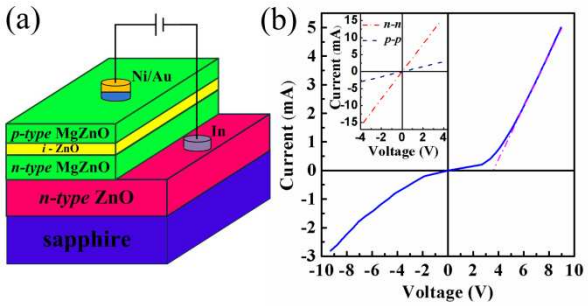

Fig. 1. (a) Schematic illustration of the *n*-$Mg_{0.13}Zn_{0.87}O$/*i*-ZnO/*p*-$Mg_{0.13}Zn_{0.87}O$ double heterostructure. (b) *I*– *V* curve of the double heterostructure, and the inset shows the *I*– *V* curves of the Ni/Au contact to the *p*-$Mg_{0.13}Zn_{0.87}O$ layer and the In contact to the *n*-ZnO layer.

The electrical properties of the ZnO films were measured in a Hall measurement system (LakeShore 7707) under Van der Pauw configuration. The structural properties of the films were characterized in a Bruker-D8 x-ray diffractometer. The composition of the MgZnO layers was determined using a VG ESCALAB MK-II X-ray photoelectron spectroscope (XPS). Photoluminescence (PL) spectra of the films were recorded employing the 325 nm line of a He-Cd laser as the excitation source. Electroluminescence (EL) measurements were carried out in a Hitachi F4500 spectrometer under the drive of a continuous current. Finite-different time-domain (FDTD) method was used to simulate the electromagnetic field distribution in the devices.

Results and discussion

The schematic diagram of the double heterostructure is shown in Fig. 1(a). Note that the *n*-$Mg_{0.13}Zn_{0.87}O$/*i*-ZnO/*p*-$Mg_{0.13}Zn_{0.87}O$ heterostructures were fabricated onto a 400 nm ZnO buffer layer. The electron concentration and Hall mobility of the buffer layer are 2.7×10^{19} cm^{-3} and 35 cm^2/Vs, respectively. An *n*-$Mg_{0.13}Zn_{0.87}O$ layer was firstly grown on the ZnO film as an electron source. The thickness of the *n*-$Mg_{0.13}Zn_{0.87}O$ layer is about 150 nm. Then a 40 nm undoped *i*-ZnO was deposited onto the *n*-$Mg_{0.13}Zn_{0.87}O$ layer as an active layer. Subsequently, a 100 nm *p*-$Mg_{0.13}Zn_{0.87}O$:(Li,N) layer was deposited on ZnO layer as the hole source layer. Indium (In) and Ni/Au were coated onto the ZnO buffer and *p*-$Mg_{0.13}Zn_{0.87}O$ layers acting as ohmic contact by thermal evaporation. The current-voltage (*I- V*) characteristic of the heterostructure shows obvious rectification behaviors with a turn-on voltage of around 3.6 V, as shown in Fig. 1(b). The inset shows that the *I- V* curves for both In contact on the *n*-ZnO and Ni/Au contact on the *p*-$Mg_{0.13}Zn_{0.87}O$, both of which are nearly beelines, indicating that ohmic contacts have been formed in both cases. The ohmic behaviors of the metal contacts exclude the possibility of the formation of any Schottky junctions in the heterostructures.

Since the optical quality of the ZnO active layers is fundamental for the performance of the heterostructure LEDs, the PL spectrum of the ZnO layer has been measured, as shown in the inset of Fig. 2. The spectrum shows a sharp peak at

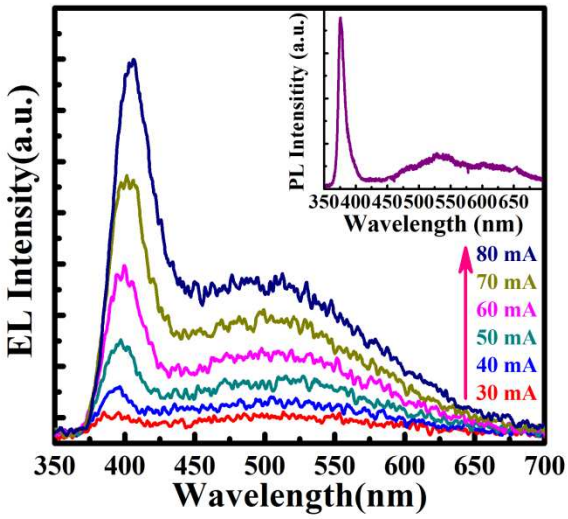

Fig. 2. Room temperature EL spectra of the double-heterostructure at different injection current, and the inset shows the room temperature PL spectra of ZnO film.

around 375 nm, which is the near-band-edge emission of ZnO, and a weak deep-level emission at around 500 nm can also be observed from the spectrum. The room temperature EL spectra of the double heterostructure are shown in Fig. 2. One can see that the emission is dominated by a band at around 400 nm, and another weak one at around 500 nm is also visible in the spectrum. The former has been commonly observed from ZnO-based LED, which can be attributed to the near-band-edge

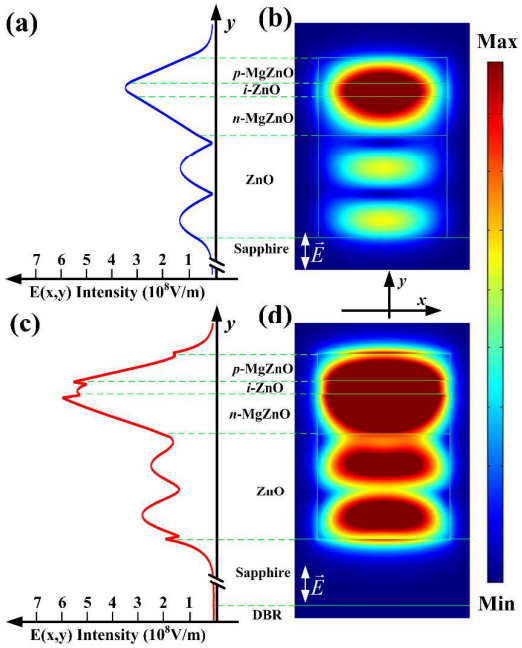

Fig. 3. The electromagnetic field distribution for the major component *E* (x,y) for the model without DBR (b) and with DBR (d); the electrical filed intensity along

the y-axis the field distributions *E* (x,y) of the fundamental mode of the device without (a) and with (c) the reflector.

emission of ZnO.[11] As for the emission at around 500 nm, it can be attributed to the deep-level related emission of ZnO.[28,29] With the increase of the injection current from 30 mA to 80 mA, the intensity of the emission at around 400nm increases significantly, and the peak of the emission redshifts from 395 nm to 405 nm. The redshift may come from the quantum confined Stark effect and/or the heating effect caused by the relatively large injection current in the structure.[30,31]

The distribution of the electromagnetic field of the emitted photons in the device has been simulated using FDTD method.[32,33] Take the effect of DBR into account, the cross section of the device with *x*-*y* plane was built to demonstrate the electromagnetic filed distribution without and with the DBR. The incident light is parallel to *y* axis, which is shown in the inset of Figs. 3(b) and 3(d). One can see from the electromagnetic field distributions E(x,y) of the *n*-$Mg_{0.13}Zn_{0.87}O$/*i*-ZnO/*p*-$Mg_{0.13}Zn_{0.87}O$ heterostructure without the DBR shown in Fig. 3(b) that the emission is mainly located in the vicinity of the *i*-ZnO layer, while only a very small portion of the emitted photons can come out of the device, and be captured by the recording detector, which means that the extraction efficiency of the LEDs is very low, and the low extraction efficiency of the emitted photons is seriously adverse to the performance of the devices. It is accepted that the major reason for the low extraction efficiency lies in the fact that the refraction index of ZnO (2.45) is much larger than that of air ambient (1.0). In such circumstance, many emitted photons will encounter total reflection and be confined into the heterostructure. Actually, how to increase the extraction efficiency has been one of the major issues for LEDs, and many strategies such as photonic crystal, textured surface, surface plasmon[34,35], *etc.* have been employed to increase the extraction efficiency of LEDs.[36-39]

To increase the extraction efficiency of ZnO LEDs, a distributed Bragg reflector (DBR) which has a relatively high reflectivity at around 400 nm (corresponding to the emission wavelength of the ZnO LEDs) has been bonded on the backside of the device, and the distribution of the emission electromagnetic field from the device with the DBR is shown in Fig. 3 (d). Compared the electromagnetic field distribution Fig. 3(b) (without the DBR) with Fig. 3(d) (with DBR), one can see that the reflector can obviously enhance electromagnetic field feedback, and the number of photons that can get out of the device and be captured by the recording detector increased significantly. The quantified enhancement of the electromagnetic field distribution curve along the *y*-axis were labelled in Figs. 3(a) (without DBR) and 3(c) (with DBR). At the same calculation condition, the electrical field intensity demonstrated obvious higher magnitude than that without the DBR at the top surface of the device. So the photons that can come out of the device and be captured by the recording detectors can be increased significantly.

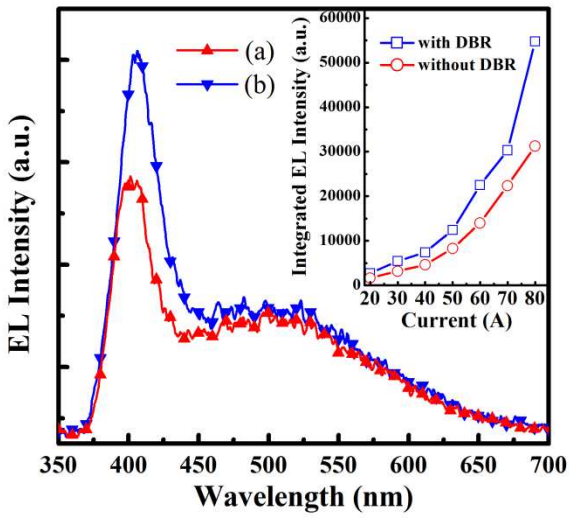

Fig. 4. The emission spectrum of the double heterostructure LEDs with (b) and without (a) the reflector. The inset shows the dependence of the integrated intensity of the emission at around 400 nm on the injection current with and without the DBR.

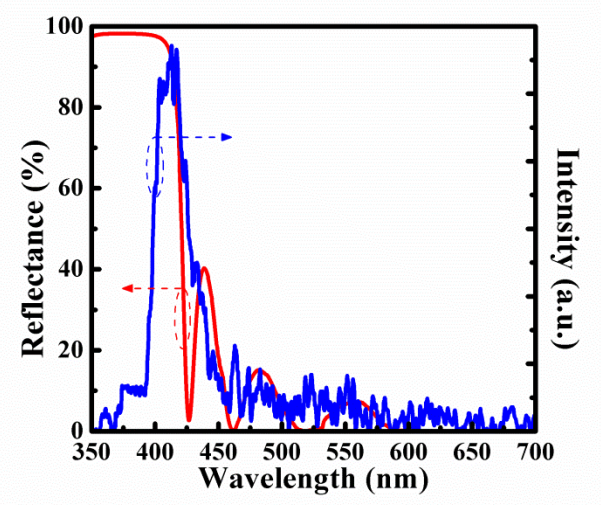

Fig. 5. The reflection spectrum of the DBR and the enhancement ratio of the device with and without the reflector by subtracting the emission intensity of the device without the reflector from that with the reflector.

To test the validity of the above simulation results, the emission of the LEDs with and without the reflector under the same injection current of 70 mA has been recorded, as shown in Fig. 4. Note that the DBR is commercial available, and is comprised by several pairs of Ta_2O_5/SiO_2. One can see from the figure that the emission of the LEDs at around 400 nm has been enhanced significantly, while that at around 500 nm changes little compared with the device without the reflector. The dependence of the integrated intensity of the emission at around 400 nm on the injection current with and without the DBR is shown in the inset of Fig. 4. One can see that the integrated intensity with the DBR is about 1.6 times larger than that without the reflector in all the investigated cases, which confirms the validity of the reflector in enhancing the emission

of the LEDs, as revealed by the simulation results shown in Fig. 3.

To understand the effect of the reflector better, the reflection spectrum of the DBR is shown in Fig. 5. One can see that the reflector shows a reflectivity of about 98% in the spectrum region at around 400 nm, while that at longer wavelength is very small. To confirm that the emission enhancement of the LEDs bonded with the DBR is caused by the reflector, the difference between the emission intensity of device with and without the reflector obtained by subtracting the emission intensity of the LEDs without the reflector from that of the LEDs with the reflector is also shown in Fig. 5. One can see that the enhancement occurs mainly in the high reflectivity region of the reflector, and the difference spectra and the reflectivity of the DBR share the same edge, which confirms that the enhancement is caused by the DBR. The above facts reveal that the extraction efficiency of the ZnO LEDs can be increased greatly by using a DBR.

Conclusions

In conclusion, *n*-$Mg_{0.13}Zn_{0.87}O$/*i*-ZnO/*p*-$Mg0_{.13}Zn_{0.87}O$ double heterostructured LEDs have been constructed, and obvious emission at around 400 nm have been obtained from the heterostructure. A DBR has been bonded backside the device to enhance the light extraction from the device, and the emission of the LEDs has been increased noticeably. FDTD method has been performed and confirmed that the reflector is effective in enhancing the emission from the top surface of the devices. The results reported in this paper may provide a route to increase the emission of ZnO-based LEDs.

Acknowledgements

This work is supported by the National Basic Research Program of China (2011CB302005), the Natural Science Foundation of China (11074248, 11104265, 11374296, and 61177040), and the Science and Technology Developing Project of Jilin Province (20111801).

Notes and references

[a] State Key Laboratory of Luminescence and Applications, Changchun Institute of Optics, Fine Mechanics and Physics, Chinese Academy of Sciences, No. 3888 Dongnanhu Road, Changchun 130033, China. Email: shancx@ciomp.ac.cn; shendz@ciomp.ac.cn.

[b] University of Chinese Academy of Sciences, Beijing 100049, China.

[c] Key Laboratory of Optical System Advanced Manufacturing Technology, Changchun Institute of Optics, Fine Mechanics and Physics, Chinese Academy of Sciences, Changchun 130033, China

1 D. C. Look, *Mat. Sci. Eng.* B, 2001, **80**, 383-387.

2 U. O□zgu□r, Y. I. Alivov, C. Liu, A. Teke, M. A. Reshchikov, S. Dog□an, V. Avrutin, S. J. Cho and H. Morkoc□, *J. Appl. Phys.*, 2005, **98**, 041301.

3 H. Dong, Y. Liu, J. Lu, Z. Chen, J. Wang and L. Zhang, *J. Mater. Chem. C*, 2013, **1**, 202-206.

4 Z. M. Bai, X. Q. Yan, X. Chen, Y. Cui, P. Lin, Y. W. Shen and Y. Zhang, RSC Adv., 2013, **3**, 17682-17688.

5 B. Panigrahy and D. Bahadur, RSC Adv., 2012, **2**, 6222.

6 A. Tsukazaki, A. Ohtomo, T. Onuma, M. Ohtani, T. Makino, M. Sumiya, K. Ohtani, S. F. Chichibu, S. Fuke, Y. Segawa, H. Ohno, H. Koinuma and M. Kawasaki, *Nat. Mater.*, 2004, **4**, 42-46.

7 S. Chu, J. H. Lim, L. J. Mandalapu, Z. Yang, L. Li and J. L. Liu, *Appl. Phys. Lett.*, 2008, **92**, 152103.

8 J. C. Sun, H. W. Liang, J. Z. Zhao, J. M. Bian, Q. J. Feng, L. Z. Hu, H. Q. Zhang, X. P. Liang, Y. M. Luo and G. T. Du, *Chem. Phys. Lett.*, 2008, **460**, 548-551.

9 Z. P. Wei, Y. M. Lu, D. Z. Shen, Z. Z. Zhang, B. Yao, B. H. Li, J. Y. Zhang, D. X. Zhao, X. W. Fan and Z. K. Tang, *Appl. Phys. Lett.*, 2007, **90**, 042113.

10 H. Shen, C. X. Shan, Q. Qiao, J. S. Liu, B. H. Li, D. Z. Shen, *J. Mater. Chem. C,* 2013, **1**, 234- 237.

11 J. S. Liu, C. X. Shan, H. Shen, B. H. Li, Z. Z. Zhang, L. Liu, L. G. Zhang and D. Z. Shen, *Appl. Phys. Lett.*, 2012, **101**, 011106.

12 Y. S. Choi, J. W. Kang, B. H. Kim, D. K. Na, S. J. Lee and S. J. Park, *Opt. express*, 2013, **21**, 11698-11704.

13 K. Nakahara, S. Akasaka, H. Yuji, K. Tamura, T. Fujii, Y. Nishimoto, D. Takamizu, A. Sasaki, T. Tanabe, H. Takasu, H. Amaike, T. Onuma, S. F. Chichibu, A. Tsukazaki, A. Ohtomo and M. Kawasaki, *Appl. Phys. Lett.*, 2010, **97**, 013501.

14 H. Zheng, Z. X. Mei, Z. Q. Zeng, Y. Z. Liu, L. W. Guo, J. F. Jia, Q. K. Xue, Z. Zhang and X. L. Du, *Thin Solid Films*, 2011, 520, 445-447.

15 Y. I. Alivov, J. E. Van Nostrand, D. C. Look, M. V. Chukichev and B. M. Ataev, *Appl. Phys. Lett.*, 2003, **83**, 2943.

16 E. Nannen, T. Kümmell, A. Ebbers and G. Bacher, *Appl. Phys. Express*, 2012, 5, 035001.

17 S. Chu, M. Olmedo, Z. Yang, J. Kong and J. Liu, *Appl. Phys. Lett.*, 2008, **93**, 181106.

18 H. Kato, T. Yamamuro, A. Ogawa, C. Kyotani and M. Sano, *Appl. Phys. Express*, 2011, **4**, 091105.

19 H. Long, S. Li, X. Mo, H. Wang, H. Huang, Z. Chen, Y. Liu and G. Fang, *Appl. Phys. Lett.*, 2013, **103**, 123504.

20 J. Y. Kong, L. Li, Z. Yang and J. L. Liu, *J. Vac. Sci. Technol.* B, 2010, **28**, C3D10-C13D12.

21 S. K. Pandey, S. Verma, S. K. Pandey and S. Mukherjee, *Int. J. Mater. Sci. Eng*., 2013, **1**, 1-4.

22 J. Lee, S. Cha, J. Kim, H. Nam, S. Lee, W. Ko, K. L. Wang, J. Park and J. Hong, *Adv. Mater.*, 2011, **23**, 4183-4187.

23 G. Li, A. Sundararajan, A. Mouti, Y. J. Chang, A. R. Lupini, S. J. Pennycook, D. R. Strachan and B. S. Guiton, *Nanoscale*, 2013, **5**, 2259-2263.

24 J. B. Yi, C. C. Lim, G. Z. Xing, H. M. Fan, L. H. Van, S. L. Huang, K. S. Yang, X. L. Huang, X. B. Qin, B. Y. Wang, T. Wu, L. Wang, H. T. Zhang, X. Y. Gao, T. Liu, A. T. S. Wee, Y. P. Feng and J. Ding, *Phys. Rev. Lett.*, 2010, **104**, 137201.

25 X. Y. Chen, Z. Z. Zhang, B. Yao, M. M. Jiang, S. P. Wang, B. H. Li, C. X. Shan, L. Liu, D. X. Zhao and D. Z. Shen, *Appl. Phys. Lett.*, 2011, **99**, 091908.

26 X. H. Wang, B. Yao, D. Z. Shen, Z. Z. Zhang, B. H. Li, Z. P. Wei, Y. M. Lu, D. X. Zhao, J. Y. Zhang, X. W. Fan, L. X. Guan and C. X. Cong, *Solid State Commun.*, 2007, **141**, 600-604.

27 J. S. Liu, C. X. Shan, B. H. Li, Z. Z. Zhang, K. W. Liu and D. Z. Shen, *Opt. Lett.*, 2013, **38**, 2113-2115.
28 F. K. Shan, G. X. Liu, W. J. Lee and B. C. Shin, *J. Appl. Phys.*, 2007, **101**, 053106.
29 S. H. Jeong, B. S. Kim and B. T. Lee, *Appl. Phys. Lett.*, 2003, **82**, 2625-2627.
30 O. Lupan, T. Pauporte and B. Viana, *Adv. Mater.*, 2010, **22**, 3298-3302.
31 H. Zhu, C. X. Shan, B. Yao, B. H. Li, J. Y. Zhang, Z. Z. Zhang, D. X. Zhao, D. Z. Shen, X. W. Fan, Y. M. Lu and Z. K. Tang, *Adv. Mater.*, 2009, **21**, 1613.
32 A. Taflove and S. C. Hagness, *Computational Electrodynamics: The Finite-Difference Time-Domain Method*, Artech House, Norwood, MA, 2000.
33 J. W. Pan, P. J. Tsai, K. D. Chang and Y. Y. Chang, *Appl. Optics*, 2013, **52**, 1358-1367.
34 Q. Qiao, C. X. Shan, J. Zheng, B. H. Li, Z. Z. Zhang, L. G. Zhang and D. Z. Shen, *J. Mater. Chem.*, 2012, **22**, 9481.
35 H. Shen, C. X. Shan, Q. Qiao, J. S. Liu, B. H. Li and D. Z. Shen, *J. Mater. Chem. C*, 2013, **1**, 234-237.
36 H. Chen, H. Guo, P. Zhang, X. Zhang, H. Liu, S. Wang and Y. Cui, *Appl. Phys. Express*, 2013, **6**, 022101.
37 H. Guo, X. Zhang, H. Chen, P. Zhang, H. Liu, H. Chang, W. Zhao, Q. Liao and Y. Cui, *Opt. Express*, 2013, **21**, 21456-21465.
38 X. Liu, W. Zhou, Z. Yin, X. Hao, Y. Wu and X. Xu, *J. Mater. Chem.*, 2012, **22**, 3916-3921.
39 J. T. Lian, J. H. Ye, J. Y. Liou, K. C. Tsao, N. C. Chen and T. Y. Lin, *J. Mater. Chem. C*, 2013, **1**, 6559-6564.

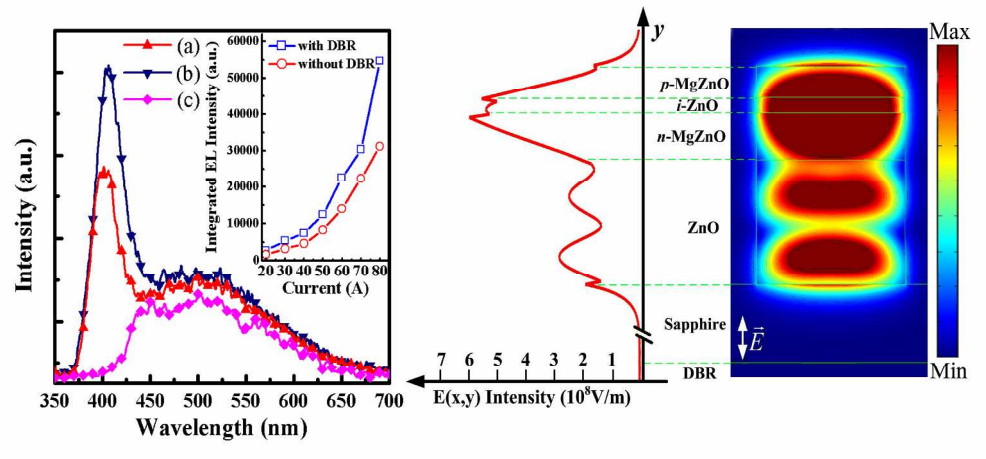

The emission of the n-Mg0.13Zn0.87O/i-ZnO/p-Mg0.13Zn0.87O heterostructure LEDs has been increased noticeably by a distributed Bragg reflector bonded backside the device.
660x305mm (150 x 150 DPI)